Rigid-Rod Polyimides Based on Noncoplanar 4,4′-Biphenyldiamines: A Review of Polymer Properties vs Configuration of Diamines

Kathy C. Chuang,*,† James D. Kinder,†,‡ Diana L. Hull,§ David B. McConville,§ and Wiley J. Youngs§

NASA Lewis Research Center, Cleveland, Ohio 44135, and Department of Chemistry, University of Akron, Akron, Ohio 44325

Received March 6, 1997; Revised Manuscript Received July 14, 1997[⊗]

ABSTRACT: X-ray crystal structures of three substituted 4,4′-biphenyldiamines, namely, 2,2′,6,6′-tetramethylbenzidine (TMBZ), 2,2′-dimethylbenzidine (DMBZ) and 2,2′-bis(trifluoromethyl)benzidine (BFBZ), were determined. The torsional angles between the two phenyl rings for TMBZ, DMBZ, and BFBZ are $\phi = 83°$, 75°, and 59°, respectively. A structure−property relationship between the three-dimensional configuration of diamine monomers and the corresponding polyimides is discussed.

Introduction

Rigid-rod polymers such as Kevlar[1] and poly(benzobis-(oxazole)),[2] are well-known for their interesting liquid crystalline behavior[3,4] and outstanding performance as high-strength, high-modulus fibers. However, rigid-rod polymers are often insoluble in common organic solvents and difficult to process. Efforts to increase the solubility of rodlike polymers have included the use of bulky substituents, kinks, crank-shaft, and noncoplanar biphenyl moieties.[5−7] Previously, polyamides[8] and polyimides containing 2,2′-substituted 4,4′-biphenyldiamine (i.e., 2,2′-substituted benzidine) have been shown to display optical transparency and improved solubility. The substitution at the 2- and 2′-positions of the biphenyl moiety appears to force the two phenyl rings into adopting a noncoplanar conformation. This, in turn, disrupts the crystal packing and provides enhanced solubility. Recently, considerable efforts in molecular modeling have been devoted to calculating the torsional angle between the two phenyl rings on either the 2,2′-substituted biphenyl[9,10] or the polyimide copolymers[11] based on 2,2′-substituted benzidines. However, to the best of our knowledge, no X-ray structure has ever been published on the noncoplanar, substituted benzidine derivatives. The purpose of this research is to investigate the correlation between physical properties of polyimides and three-dimensional structures of the corresponding diamine monomers, i.e., noncoplanar, substituted benzidines. Property−structure relationships, such as glass transition temperature (T_g) and solubility of polyimides *versus* X-ray crystal structures of the corresponding substituted benzidines, will be explored. Hopefully, information about the torsional angle between the two phenyl rings and the placement of the substituents on benzidine will provide some insights complementary to the results of molecular modeling on these polymers.

Thermoplastic polyimides, prepared from 2,2′-dimethylbenzidine, 2,2′-bis(trifluoromethyl)benzidine, and 2,2′,6,6′-tetramethylbenzidine with various aromatic dianhydrides in a high boiling solvent, such as *m*-cresol, had high molecular weight and could be spun into high-strength, high-modulus fibers.[12] Furthermore, these polyimides also exhibited excellent thermal stability, low coefficients of thermal expansion (CTE) and low dielectric constants, suitable for electronic packaging.[13−15] Thermosetting polyimides derived from 4,4′-(hexafluoroisopropyliene)diphthalic anhydride (HFDA) and 2,2′,6,6′-tetramethylbenzidine exhibited higher T_g's than the corresponding polyimides containing 2,2′-bis(trifluoromethyl)benzidine.[16,17] This article will relate the properties of thermoplastic polyimides, derived from 2,2′-dimethylbenzidine (DMBZ), 2,2′-bis(trifluoromethyl) benzidine (BFBZ), and 2,2′,6,6′-tetramethylbenzidine (TMBZ), to the X-ray crystal structures of these three substituted benzidines.

Experimental Section

Materials. All the dianhydrides, 2,2′-bis(trifluoromethyl)-benzidine, and 2,2′-dimethylbenzidine (i.e., *m*-tolidine, received as dihydrochlorides) used in this study were purchased from Chriskev Co., Inc. The dianhydrides were dried at 150 °C under vacuum prior to use. 2,2′,6,6′-Tetramethylbenzidine was synthesized following a reported procedure.[17] The *m*-cresol, obtained from Aldrich Chemical Co., was distilled from phosphorus pentaoxide under vacuum.

Polymer Synthesis and Sample Preparation. The polymerization[18] (Figure 1) was accomplished by reacting a dianhydride, such as 3,3′,4,4′-biphenyltetracarboxylic dianhydride (BPDA), with a selected 4,4′-biphenyldiamine (either TMBZ, DMBZ, or BFBZ) in *m*-cresol overnight at room temperature to form the poly(amic acid). Isoquinoline (1 wt %) was added initially as a catalyst. The poly(amic acid) was then heated to reflux for 6 h to afford the corresponding polyimides. However, certain polyimides precipitated out prematurely, depending on the substituted benzidine used in the polymerization. No further characterization was attempted on these precipitated polyimides. The TMBZ−BPDA and BFBZ−BPDA fibers were produced from an isotropic solution of 10% (w/w) polyimides in *m*-cresol, via a dry-jet wet spinning process into a coagulation bath of water/acetone.[19] The as-spun fibers, which had little tensile strength, were then drawn at an elevated temperature (>400 °C) up to 6 to 10 times draw ratio in air by a zone drawing method. An exception, DMBZ−BPDA was polymerized and spun from *p*-chlorophenol as reported in the literature.[20] The single crystals of TMBZ, DMBZ, and BFBZ were obtained by recrystallization from benzene and petroleum ether.

X-ray Crystallography. Crystallographic data for the three substituted benzidines (TMBZ, DMBZ, BFBZ) were

* To whom corespondence should be addressed.
† NASA Lewis Research Center.
‡ Postdoctor fellow of National Research Council (1992−1995). Present address: Ferro Corp., Cleveland, OH 44131.
§ University of Akron.
⊗ Abstract published in *Advance ACS Abstracts,* October 15, 1997.

S0024-9297(97)00309-4 CCC: $14.00

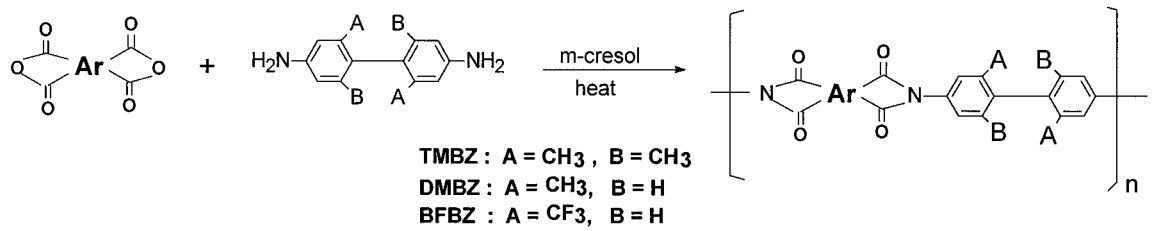

Figure 1. Polyimide synthesis.

collected at low temperature using a Syntex $P2_1$ diffractometer employing Mo Kα radiation ($\lambda = 0.710\ 71$ Å). Intensity data for each were collected between 3.5° and 50.0° in 2θ using the ω scan technique at 8.37 deg/min^{-1} with a scan range of 2.00°. TMBZ ($C_{16}H_{20}N_{22}$, white parellpiped) formed in monoclinic space group $P2_1/c$ with 13 formula units per unit cell: a = 11.366(2) Å, b = 16.533(3) Å, c = 22.424(4) Å, $\alpha = \gamma = 90°$, β = 100.05(3)°, V = 4149.2(1) Å^3, density (calculated) = 1.154 Mg/m^3, as determined from reflections in the 2θ range of 3.5° to 45.0° at 105 K. The asymmetric unit cell contained three independent molecules. DMBZ ($C_{14}H_{16}N_2$) crystallized in the orthorhombic space group *Pbca* (#61) with 8 formula units per unit cell: a = 14.580(3) Å, b = 7.502(3) Å, c = 21.133(5) Å, $\alpha = \beta = \gamma = 90°$, V = 2311.4(1) Å^3, density (calculated) = 1.220 Mg/m^3, determined from 25 reflections in the 2θ range of 20° to 30° at 157 K. BFBZ ($C_{14}H_{10}N_2F_6$) solved in the orthorhombic space group *Pbcn* (#60) with 4 formula units per unit cell: a = 12.937(3) Å, b = 5.847(1) Å, c = 17.649(4) Å, $\alpha = \beta = \gamma = 90°$, V = 1334.9(5) Å^3, density (calculated) = 1.593 Mg/m^3, as deduced from 29 reflections in the 2θ range of 20° to 30° at 139 K. All the structures were solved by direct methods using the SHELXTL PLUS program set.[24] All non-hydrogen atoms were located from the initial E-maps and refined by full-matrix least squares on F^2 using the program SHELXL-93.[25] Corrections for the effects of primary and secondary extinction were applied (extinction coefficient = 0.0006(2) for TMBZ, 0.019(2) for DMBZ, and 0.010(2) for BFBZ).[26] All hydrogen atoms, with the exception of those of the amino groups, were placed in idealized positions and refined using a riding model. The amino hydrogen atoms were located from the difference-Fourier maps for both compounds. The TMBZ coordinates of amino hydrogen's were refined *via* a riding model. Refinement to convergence of 488 parameters on 3858 unique data (R_{int} = 0.0188) afforded a weighted discrepancy index[27] of 7.98% (R = 6.54% for 3858 data with $F_0^2 > 4\sigma(F_0^2)$),[28] and a goodness-of-fit[29] of 2.14). For DMBZ, refinement to convergence of 160 parameters on 1829 unique data (R_{int} = 0.0169) yielded a weighted R factor[27] of 7.28% (R = 3.43% for 1265 data with $F_0^2 > 4\sigma(F_0^2)$) and a goodness-of-fit of 1.012 for DMBZ. For BFBZ, 101 parameters were refined against 1171 unique data (R_{int} = 0.0277) to produce a weighted R factor of 7.18% (R = 2.98% for 833 data *with* $F_0^2 > 4\sigma\ (F_0)^2$ and a goodness-of-fit of 1.002).

Inspection of the difference-Fourier maps for DMBZ showed some disorder of the methyl groups. These groups were refined as an ideally disordered rotor in which one part of the disordered group is offset from the other by 60°. The site occupation factor of one part was set equal to a free variable while the site occupancy of the other was set to one minus that free variable. This treatment gave site occupation factor for the primary parts of 71.7% for C(13) and 66.3% for C(14). the isoptropic U values of both parts were set equal to 1.5 times that of the carbon atom. The trifluoromethyl group of BFBZ, however, showed no evidence of rotational disorder with largest U_{eq} value being that of F(2) at 1.7 times the value of C(7).

The phenyl rings in each compound are rotated about the joining sigma (σ) bond. The angle between the least-squares planes as defined by the phenyl ring carbon atoms in TMBZ, DMBZ, and BFBZ are 83°, 75°, and 59°. The structure determination summaries for TMBZ, DMBZ, and BFBZ are listed in Table 1, Table 2, and Table 3, respectively. Other X-ray crystallography information concerning the atomic coordinates and equivalent isotropic displacement coefficients, bond lengths, and bond angles are listed in Tables 4−6 for TMBZ, Tables 7−9 for DMBZ, and Tables 10−12 for BFBZ. Additional X-ray crystallography data such as anisotropic displacement coefficients, H-atom coordinates, and isotropic displacement as well as observed and calculated structure factors are available as Supporting Information.

Results and Discussion

As shown in the X-ray structure, the torsional angle between the two phenyl rings of TMBZ is ϕ = 83° (Figure 2), compared to that of ϕ = 75° for DMBZ (Figure 3) and ϕ = 59° for BFBZ (Figure 4). However, the difference in torsional angle did not seem to have any effect on the chemical shifts (Table 14) of ^{13}C-NMR spectra of TMBZ, DMBZ, and BFBZ (Figure 5) as well

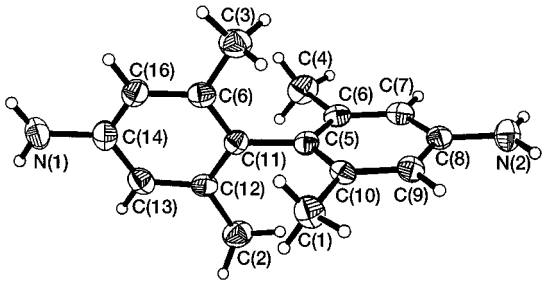

Figure 2. Molecular configuration of 2,2′,6,6′-tetramethylbenzidine (TMBZ).

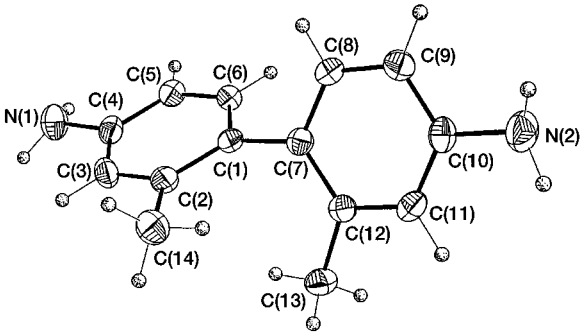

Figure 3. Molecular configuration of 2,2′-dimethylbenzidine (DMBZ).

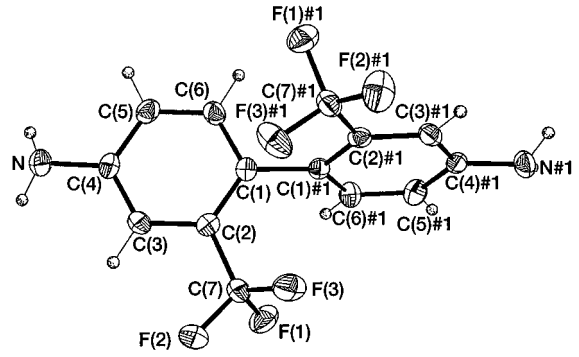

Figure 4. Molecular configuration of 2,2′-bis(trifluoromethyl)-benzidine (BFBZ).

Table 1. Structure Determination Summary for TMBZ

Crystal Data					
empirical formula	$C_{16}H_{20}N_2$	unit cell dimensions	$a = 11.366(2)$ Å	volume	4149.2(13) Å^3
color; habit	white parellpiped		$b = 16.533(3)$ Å	Z	13
crystal size (mm)	0.3 × 0.3 × 0.5		$c = 22.424(4)$ Å	formula weight	221.9
crystal	system monoclinic		$\beta = 100.05(3)$ Å	density (calcd)	1.154 Mg/m^3
space group	$P2_1/c$			absorption coefficient	0.064 mm^{-1}
				$F(000)$	1560

Data Collection			
diffractometer used	Siemens R3m/V	standard reflections	3 measured every 97 reflections
radiation	Mo Kα ($\lambda = 0.710\ 73$ Å)	index ranges	$-12 \le h \le 0$, $0 \le k \le 17$, $-23 \le l \le 24$
temperature (K)	103	reflections collected	5739
monochromator	highly oriented graphite crystal	independent reflections	5418 ($R_{int} = 1.88\%$)
2θ range	3.5−45.0°	observed reflections	3858 ($F > 4.0\sigma(F)$)
scan type	ω	absorption correction	N/A
scan speed constant	0.50 deg/min in ω		
scan range (ω)	0.50°		
background measurement	stationary crystal and stationary counter at beginning and end of scan, each for 12.5% of total scan time		

Solution and Refinement			
system used	SHELXTL PLUS (PC Version)	no. of parameters refined	488
solution	direct methods	final R indices (obsd data)	$R = 6.47\%$, wR = 7.50%
refinement method	full-matrix least squares	R indices (all data)	R 9.26%, wR = 7.88%
quantity minimized	$\sum w(F_o - F_c)^2$	goodness-of-fit	2.09
absolute structure	N/A	largest and mean Δ/σ	0.032, 0.006
extinction correction	$\chi = 0.0006\ (2)$, where $F^* = F[1 + 0.002\chi F^2/\sin(2\theta)]^{-1/4}$	data-to-parameter ratio	7.9:1
hydrogen atoms	riding model, fixed isotropic U	largest difference peak	0.48 e Å^{-3}
weighting scheme	$w^{-1} = \sigma^2(F) + 0.0004F^2$	largest difference hole	−0.33 e Å^{-3}

Table 2. Crystal Data and Structure Refinement for DMBZ

empirical formula: $C_{14}H_{16}N_2$
formula weight: 212.29
temperature: 157 K
wavelength: 0.717073 Å
crystal system: orthorhombic
space group: *Pbca*
unit cell dimensions $a = 14.580(3)$ Å, α = 90°
$b = 7.502(3)$ Å, $\beta = 90°$
$c = 21.133(5)$ Å, $\gamma = 90°$
volume, Z: 2311.4(10) Å^3, 8
density (calculated): 1.220 Mg/m^3
absorption coefficient: 0.073 mm^{-1}
$F(000)$: 912
crystal size: 0.58 × 0.52 × 0.24 mm

diffractometer used: Syntex $P2_1$
monochromator: highly oriented graphite crystal
scan type: ω
scan range: 2.00°
scan speed: constant; 8.37 deg/min in ω
background measurement: stationary crystal and stationary counter at beginning and end of scan, each for 25% of total scan time
standard reflections: 3 measured every 97 reflections
range for data collection: 1.93 to 24.07°
limiting indices: $-1 \le h \le 16$, $-1 \le k \le 8$, $-24 \le l \le 1$
reflections collected: 2442
independent reflections: 1829 [$R_{int} = 0.0169$]

program set: SHELXTL PLUS Version 5γ
structure solution: Direct methods
refinement program: SHELXTL-93 (Sheldrick, G. M. *SHELXL-93 Program for the refinement of crystal structures.* Univ of Gottingen, Germany, 1993)
refinement method: full-matrix least squares on F^2
hydrogen atom location: all H atoms were placed in idealized positions except those of the amino groups which werer located from difference-Fourier maps
hydrogen atom treatment: Hydrogen atoms were refined using a riding model with isotropic U values fixed at 1.2 times (for aryl) and 1.5 times (for amino and methyl) the U_{eq} of the previous normal atom. The methyl groups were modeled as ideally disordered rigid rotors. The site occupancy of one set of hydrogens was set equal to a free variable while the other group was set equal to one minus that free variable. The coordinates of the amino hydrogen atoms were allowed to refine independently of the corresponding nitrogen atoms.
Data/restraints/parameters: 1829/0/160
goodness-of-fit on F^2: 1.012
weighting scheme: $w = 1/[\sigma^2(F_o^2) + (0.0320P)^2 + 0.0000P]$, where $P = (F_o^2 + 2F_c^2)/3$
final R indices [$I > 2\sigma I$]: R1 = 0.0343, wR2 = 0.0704
R indices (all data): R1 = 0.0518, wR2 = 0.0728
extinction coefficient: 0.019(2)
extinction expression: $F_c^* = kF_c[1 + 0.001F_c^2\lambda^3/\sin(2\theta)]^{-1/4}$
shift/esd max and mean: 0.000 and 0.000
largest diff peak and hole: 0.173 and −0.142 e Å^{-3}
refinement details: Refinement was performed on F^2 for all reflections. Weighted R-factors, wR2, and all goodnesses of fit, S, are based on F^2, and conventional R-factors, R1, are based on F, with F set to zero for negative F^2. The observed criterion of $I > 2\sigma I$ is used only for calculating the observed R factor and is not relevant to the choice of reflections used in refinement. R-factors based on F^2 are statistically about twice as large as those based on F, and R-factors based on all data will be even larger.

Table 3. Crystal Data and Structure Refinement for BFBZ

empirical formula: $C_{14}H_{10}F_6N_2$
formula weight: 320.24
temperature: 139 K
wavelength: 0.71073 Å (Mo Kα)
crystal system: orthorhombic
unit cell dimensions: $a = 12.937(3)$ Å
$b = 5.8467(14)$ Å
$c = 17.649(4)$ Å
volume, Z: 1334.9(5) Å^3, 4
space group: *Pbcn*
density (calculated): 1.593 Mg/m^3
absorption coefficient: 0.154 mm^{-1}
$F(000)$: 648
crystal size: 0.64 × 0.36 × 0.2 mm

diffractometer used: Syntex $P2_1$
monochromator: Highly oriented graphite crystal
scan type: ω
scan range: 2.00°
scan speed: constant; 8.37°/min in ω
background measurement: stationary crystal and stationary counter at beginning and end of scan, each for 25% of total scan time
standard reflections: 3 measured every 97 reflections
theta range for data collection: 2.31 to 24.98°
limiting indices: $-1 \le h \le 15$, $-1 \le k \le 6$, $-20 \le l \le 1$
reflections collected: 1631
independent reflections: 1171 [$R_{int} = 0.0277$]

program set: SHELXTL PLUS Version 5γ
structure solution: direct methods
refinement program: SHELXTL-93 (Sheldrick, G.M. *SHELXTL-93 Program for the refinement of crystal structures*. Univ of Gottingen, Germany, 1993)
refinement method: full-matrix least squares on F^2
hydrogen atom location: all H atoms were placed in idealized positions except those of the amino group which were located from difference-Fourier maps
hydrogen atom treatment: Aryl hydrogen atoms were refined using a riding model with isotropic U values fixed at 1.2 times the U_{eq} of the previous normal atom. The amino hydrogen atoms were also allowed to ride but the isotropic U values were held fixed.
data/restraints/parameters: 1171/0/101
goodness-of-fit on F^2: 1.002
weighting scheme: $w = 1/[\sigma^2(F_o^2) + (0.0350P)^2 + 0.0000P]$ where $P = (F_o^2 + 2F_c^2)/3$
final R indices [$I > 2\sigma I$)]: R1 = 0.0298, wR2 = 0.0692
R indices (all data): R1 = 0.0476, wR2 = 0.0718
extinction coefficient: 0.010(2)
extinction expression: $F_c^* = kF_c[1 + 0.001F_c^2\lambda^3/\sin(2\theta)]^{-1/4}$
shift/esd max and mean: 0.002 and 0.000
largest diff peak and hole: 0.165 and −0.157 e Å^{-3}
refinement details: Refinement was performed on F^2 for all reflections. Weighted R-factors, wR2, and all goodnesses of fit, S, are based on F^2, and conventional R-factors, R1, are based on F, with F set to zero for negative F^2. The observed criterion of $I > 2\sigma I$ is used only for calculating the observed R factor and is not relevant to the choice of reflections used in refinement. R-factors based on F^2 are statistically about twice as large as those based on F, and R-factors based on all data will be even larger.

Table 4. Atomic Coordinates (×10^5) and Equivalent Isotropic Displacement Coefficients (Å^2 × 10^4) for TMBZ

	x	y	z	U(eq)[a]		x	y	z	U(eq)[a]
N(1)	45 152 (34)	57 615 (26)	−40 545 (17)	464 (16)	C(6A)	−4 099 (37)	52 684 (25)	35 501 (19)	254 (15)
N(2)	58 609 (34)	89 742 (22)	−2 631 (16)	377 (15)	C(7A)	−5 232 (36)	50 185 (26)	24 383 (18)	237 (15)
N(1A)	−24 585 (30)	50 863 (22)	6 576 (15)	327 (14)	C(8A)	−10 527 (38)	43 228 (25)	21 670 (19)	268 (16)
N(2A)	20 891 (34)	52 303 (23)	48 514 (16)	391 (15)	C(9A)	−16 859 (37)	43 492 (26)	15 800 (19)	261 (16)
N(1B)	−55 039 (30)	12 986 (24)	49 303 (17)	398 (15)	C(10A)	−18 033 (35)	50 596 (25)	12 507 (18)	233 (15)
N(2B)	26 554 (30)	27 712 (22)	43 656 (16)	336 (14)	C(11A)	−12 679 (36)	57 530 (25)	15 198 (19)	269 (16)
C(2)	53 537 (37)	74 831 (27)	−30 084 (20)	291 (16)	C(12A)	−6 300 (36)	57 426 (25)	21 075 (19)	240 (15)
C(3)	50 908 (36)	70 227 (29)	−35 365 (21)	327 (17)	C(13A)	20 030 (40)	45 435 (29)	27 015 (20)	382 (18)
C(4)	47 487 (38)	62 169 (30)	−35 168 (21)	339 (18)	C(14A)	−9 608 (48)	35 309 (26)	25 035 (21)	448 (19)
C(5)	46 741 (38)	58 722 (28)	−29 602 (21)	330 (17)	C(15A)	−17 176 (38)	54 662 (29)	34 313 (21)	359 (18)
C(6)	49 067 (38)	63 234 (28)	−24 267 (21)	305 (17)	C(16A)	−685 (40)	65 197 (25)	23 717 (20)	350 (17)
C(7)	54 258 (38)	76 423 (24)	−18 894 (19)	252 (15)	C(1B)	−19 399 (35)	18 201 (24)	48 014 (18)	210 (14)
C(8)	64 991 (37)	76 113 (26)	−14 753 (19)	261 (16)	C(2B)	−26 064 (36)	12 850 (25)	43 910 (18)	232 (15)
C(9)	66 223 (38)	80 566 (26)	−9 418 (19)	284 (16)	C(3B)	−37 731 (37)	10 892 (26)	44 479 (19)	275 (16)
C(10)	57 084 (39)	85 387 (25)	−8 104 (19)	277 (16)	C(4B)	−43 009 (36)	14 406 (26)	49 028 (20)	283 (16)
C(11)	46 584 (38)	85 954 (25)	−12 328 (20)	298 (17)	C(5B)	−36 259 (36)	19 578 (25)	53 128 (19)	251 (15)
C(12)	45 105 (38)	81 542 (26)	−17 653 (20)	286 (16)	C(6B)	−24 538 (35)	21 442 (25)	52 725 (18)	219 (15)
C(13)	57 781 (43)	83 441 (29)	−30 469 (21)	426 (19)	C(7B)	−7 251 (36)	20 757 (25)	47 122 (18)	236 (15)
C(14)	75 428 (38)	71 189 (29)	−16 078 (21)	381 (18)	C(8B)	3 071 (35)	16 870 (25)	50 015 (18)	224 (15)
C(15)	47 787 (44)	59 251 (29)	−18 399 (21)	416 (19)	C(9B)	14 107 (36)	19 307 (25)	48 887 (18)	232 (15)
C(1)	52 428 (35)	71 391 (26)	−24 514 (19)	253 (16)	C(10B)	15 214 (37)	25 476 (26)	44 818 (19)	257 (15)
C(16)	33 430 (38)	82 224 (30)	−22 022 (22)	429 (19)	C(11B)	4 986 (37)	29 599 (26)	42 118 (18)	261 (15)
C(1A)	1 583 (37)	50 225 (23)	30 780 (19)	226 (15)	C(12B)	−6 182 (37)	27 278 (25)	43 224 (18)	241 (15)
C(2A)	13 647 (38)	48 182 (24)	32 034 (19)	250 (16)	C(13B)	−20 924 (39)	9 210 (27)	38 721 (19)	319 (16)
C(3A)	19 993 (39)	48 662 (24)	37 926 (19)	279 (16)	C(14B)	2 372 (39)	10 082 (26)	54 449 (20)	322 (16)
C(4A)	14 360 (40)	51 328 (25)	42 632 (20)	290 (17)	C(15B)	−17 564 (37)	27 172 (26)	57 261 (20)	315 (16)
C(5A)	2 393 (40)	53 271 (26)	41 355 (20)	304 (17)	C(16B)	−17 155 (39)	31 826 (27)	40 271 (20)	354 (17)

[a] Equivalent isotropic U defined as one-third of the trace of the orthogonalized $\mathbf{U}_{ij}$ tensor.

Table 5. Bond Length (Å) for TMBZ

N(1)−C(4)	1.407(6)	C(7)−C(8)	1.399(5)	C(4A)−C(5A)	1.378(6)	C(2B)−C(3B)	1.392(6)
N(2)−C(10)	1.407(6)	C(7)−C(12)	1.406(6)	C(5A)−C(6A)	1.392(6)	C(2B)−C(13B)	1.515(6)
N(1A)−C(10A)	1.407(5)	C(7)−C(1)	1.494(6)	C(6A)−C(15A)	1.500(6)	C(3B)−C(4B)	1.397(7)
N(2A)−C(4A)	1.405(5)	C(8)−C(9)	1.391(6)	C(7A)−C(8A)	1.388(6)	C(4B)−C(5B)	1.385(6)
N(1B)−C(4B)	1.399(6)	C(8)−C(14)	1.510(6)	C(7A)−C(12A)	1.402(6)	C(5B)−C(6B)	1.386(6)
N(2B)−C(10B)	1.408(6)	C(9)−C(10)	1.381(6)	C(8A)−C(9A)	1.386(6)	C(6B)−C(15B)	1.510(6)
C(2)−C(3)	1.396(6)	C(10)−C(11)	1.391(6)	C(8A)−C(14A)	1.506(6)	C(7B)−C(8B)	1.394(5)
C(2)−C(13)	1.510(7)	C(11)−C(12)	1.384(6)	C(9A)−C(10A)	1.381(6)	C(7B)−C(12B)	1.407(6)
C(2)−C(1)	1.398(6)	C(12)−C(16)	1.510(6)	C(10A)−C(11A)	1.386(6)	C(8B)−C(9B)	1.382(6)
C(3)−C(4)	1.391(7)	C(1A)−C(2A)	1.392(6)	C(11A)−C(12A)	1.389(6)	C(8B)−C(14B)	1.511(6)
C(4)−C(5)	1.388(7)	C(1A)−C(6A)	1.393(6)	C(12A)−C(16A)	1.509(6)	C(9B)−C(10B)	1.389(6)
C(5)−C(6)	1.395(6)	C(1A)−C(7A)	1.507(5)	C(1B)−C(2B)	1.400(5)	C(10B)−C(11B)	1.392(6)
C(6)−C(15)	1.501(7)	C(2A)−C(3A)	1.393(6)	C(1B)−C(6B)	1.400(6)	C(11B)−C(12B)	1.389(6)
C(6)−C(1)	1.405(6)	C(2A)−C(13A)	1.511(7)	C(1B)−C(7B)	1.490(6)	C(12B)−C(16B)	1.507(6)
		C(3A)−C(4A)	1.398(7)				

Table 6. Bond Angles (deg) for TMBZ

C(3)−C(2)−C(13)	119.3(4)	C(2A)−C(1A)−C(6A)	119.2(4)	C(2B)−C(1B)−C(6B)	119.3(4)
C(3)−C(2)−C(1)	119.8(4)	C(2A)−C(1A)−C(7A)	121.1(4)	C(2B)−C(1B)−C(7B)	119.9(4)
C(13)−C(2)−C(1)	120.9(4)	C(6A)−C(1A)−C(7A)	119.7(4)	C(6B)−C(1B)−C(7B)	120.7(3)
C(2)−C(3)−C(4)	121.0(4)	C(1A)−C(2A)−C(3A)	120.4(4)	C(1B)−C(2B)−C(3B)	120.1(4)
N(1)−C(4)−C(3)	119.8(4)	C(1A)−C(2A)−C(13A)	120.4(4)	C(1B)−C(2B)−C(13B)	121.3(4)
N(1)−C(4)−C(5)	121.3(4)	C(3A)−C(2A)−C(13A)	119.2(4)	C(3B)−C(2B)−C(13B)	118.6(4)
C(3)−C(4)−C(5)	118.9(4)	C(2A)−C(3A)−C(4A)	120.3(4)	C(2B)−C(3B)−C(4B)	120.5(4)
C(4)−C(5)−C(6)	121.3(4)	N(2A)−C(4A)−C(3A)	120.5(4)	N(1B)−C(4B)−C(3B)	120.7(4)
C(5)−C(6)−C(15)	119.0(4)	N(2A)−C(4A)−C(5A)	120.6(4)	N(1B)−C(4B)−C(5B)	120.4(4)
C(5)−C(6)−C(1)	119.4(4)	C(3A)−C(4A)−C(5A)	118.8(4)	C(3B)−C(4B)−C(5B)	118.9(4)
C(15)−C(6)−C(1)	121.6(4)	C(4A)−C(5A)−C(6A)	121.4(4)	C(4B)−C(5B)−C(6B)	121.4(4)
C(8)−C(7)−C(12)	118.7(4)	C(1A)−C(6A)−C(5A)	119.8(4)	C(1B)−C(6B)−C(5B)	119.8(4)
C(8)−C(7)−C(1)	121.1(4)	C(1A)−C(6A)−C(15A)	120.3(4)	C(1B)−C(6B)−C(15B)	120.6(4)
C(12)−C(7)−C(1)	120.2(4)	C(5A)−C(6A)−C(15A)	119.9(4)	C(5B)−C(6B)−C(15B)	119.6(4)
C(7)−C(8)−C(9)	119.8(4)	C(1A)−C(7A)−C(8A)	122.2(4)	C(1B)−C(7B)−C(8B)	122.1(4)
C(7)−C(8)−C(14)	120.9(4)	C(1A)−C(7A)−C(12A)	118.9(4)	C(1B)−C(7B)−C(12B)	118.9(3)
C(9)−C(8)−C(14)	119.3(4)	C(8A)−C(7A)−C(12A)	119.0(4)	C(8B)−C(7B)−C(12B)	119.0(4)
C(8)−C(9)−C(10)	121.5(4)	C(7A)−C(8A)−C(9A)	120.2(4)	C(7B)−C(8B)−C(9B)	119.8(4)
N(2)−C(10)−C(9)	119.9(4)	C(7A)−C(8A)−C(14A)	120.9(4)	C(7B)−C(8B)−C(14B)	120.8(4)
N(2)−C(10)−C(11)	121.3(4)	C(9A)−C(8A)−C(14A)	118.8(4)	C(9B)−C(8B)−C(14B)	119.4(3)
C(9)−C(10)−C(11)	118.8(4)	C(8A)−C(9A)−C(10A)	121.3(4)	C(8B)−C(9B)−C(10B)	121.6(4)
C(10)−C(11)−C(12)	120.8(4)	N(1A)−C(10A)−C(9A)	121.2(4)	N(2B)−C(10B)−C(9B)	120.3(4)
C(7)−C(12)−C(11)	120.3(4)	N(1A)−C(10A)−C(11A)	120.4(4)	N(2B)−C(10B)−C(11B)	120.9(4)
C(7)−C(12)−C(16)	120.9(4)	C(9A)−C(10A)−C(11A)	118.5(4)	C(9B)−C(10B)−C(11B)	118.7(4)
C(11)−C(12)−C(16)	118.8(4)	C(10A)−C(11A)−C(12A)	121.3(4)	C(10B)−C(11B)−C(12B)	120.5(4)
C(2)−C(1)−C(6)	119.5(4)	C(7A)−C(12A)−C(11A)	119.7(4)	C(7B)−C(12B)−C(11B)	120.2(4)
C(2)−C(1)−C(7)	120.4(4)	C(7A)−C(12A)−C(16A)	121.8(3)	C(7B)−C(12B)−C(16B)	120.1(4)
C(6)−C(1)−C(7)	120.0(4)	C(11A)−C(12A)−C(16A)	118.5(4)	C(11B)−C(12B)−C(16B)	119.7(4)

Table 7. Atomic Coordinates (×10⁴) and Equivalent Isotropic Displacement Parameters (Å² × 10³) for DMBZ[a]

	x	*y*	*z*	U_{eq}
N(1)	3473(1)	−1890(2)	5548(1)	39(1)
N(2)	3597(1)	883(2)	953(1)	38(1)
C(1)	3695(1)	−620(2)	3603(1)	23(1)
C(2)	3884(1)	672(2)	4067(1)	26(1)
C(3)	3834(1)	200(2)	4702(1)	30(1)
C(4)	3584(1)	−1496(2)	4901(1)	28(1)
C(5)	3377(1)	−2764(2)	4443(1)	28(1)
C(6)	3439(1)	−2322(2)	3811(1)	26(1)
C(7)	3712(1)	−229(2)	2912(1)	23(1)
C(8)	2913(1)	−476(2)	2559(1)	28(1)
C(9)	2866(1)	−124(2)	1921(1)	31(1)
C(10)	3630(1)	534(2)	1608(1)	27(1)
C(11)	4439(1)	727(2)	1945(1)	27(1)
C(12)	4499(1)	341(2)	2587(1)	23(1)
C(13)	5424(1)	473(2)	2903(1)	33(1)
C(14)	4070(1)	2596(2)	3903(1)	37(1)

[a] U_{eq} is defined as one-third of the trace of the orthogonalized $\mathbf{U}_{ij}$ tensor.

Table 8. Bond Lengths (Å) and Angles (deg) for DMBZ[a]

N(1)−C(4)	1.406(2)	C(7)−C(12)	1.403(2)
N(2)−C(10)	1.410(2)	C(8)−C(9)	1.375(2)
C(1)−C(6)	1.401(2)	C(9)−C(10)	1.386(2)
C(1)−C(2)	1.406(2)	C(10)−C(11)	1.385(2)
C(1)−C(7)	1.489(2)	C(11)−C(12)	1.390(2)
C(2)−C(3)	1.389(2)	C(12)−C(13)	1.509(2)
C(2)−C(14)	1.509(2)	N(1)−H(2A)#1	2.34(2)
C(3)−C(4)	1.389(2)	N(2)−H(1B)#3	2.17(2)
C(4)−C(5)	1.391(2)	H(1B)−N(2)#4	2.17(2)
C(5)−C(6)	1.379(2)	H(2A)−N(1)#2	2.34(2)
C(7)−C(8)	1.397(2)		
C(6)−C(1)−C(2)	117.4(1)	C(8)−C(7)−C(12)	117.4(1)
C(6)−C(1)−C(7)	119.5(1)	C(8)−C(7)−C(1)	119.0(1)
C(2)−C(1)−C(7)	123.0(1)	C(12)−C(7)−C(1)	123.6(1)
C(3)−C(2)−C(1)	119.2(1)	C(9)−C(8)−C(7)	122.7(2)
C(3)−C(2)−C(14)	118.3(1)	C(8)−C(9)−C(10)	119.7(2)
C(1)−C(2)−C(14)	122.3(1)	C(11)−C(10)−C(9)	118.4(1)
C(4)−C(3)−C(2)	122.7(2)	C(11)−C(10)−N(2)	120.9(2)
C(3)−C(4)−C(5)	118.2(1)	C(9)−C(10)−N(2)	120.5(2)
C(3)−C(4)−N(1)	121.2(2)	C(10)−C(11)−C(12)	122.2(2)
C(5)−C(4)−N(1)	120.5(2)	C(11)−C(12)−C(7)	119.3(1)
C(6)−C(5)−C(4)	119.7(2)	C(11)−C(12)−C(13)	118.3(1)
C(5)−C(6)−C(1)	122.7(2)	C(7)−C(12)−C(13)	122.3(1)

[a] Symmetry transformations used to generate equivalent atoms: #1 = 0.5 − *x*, −*y*, 0.5 + *z*; #2 = 0.5 − *x*, −*y*, −0.5 + *z*; #3 = *x*, −0.5 − *y*, −0.5 + *z*; #4 = *x*, −0.5 − *y*, 0.5 + *z*.

Table 9. Torsion Angles (deg) for DMBZ

C(6)−C(1)−C(2)−C(3)	1.7(2)	C(4)−C(5)−C(6)−C(1)	−0.7(2)	C(8)−C(9)−C(10)−C(11)	3.4(2)
C(7)−C(1)−C(2)−C(3)	178.7(1)	C(2)−C(1)−C(6)−C(5)	−0.7(2)	C(8)−C(9)−C(10)−N(2)	179.3(2)
C(6)−C(1)−C(2)−C(14)	−173.5(1)	C(7)−C(1)−C(6)−C(5)	−177.8(1)	C(9)−C(10)−C(11)−C(12)	−2.2(2)
C(7)−C(1)−C(2)−C(14)	3.5(2)	C(6)−C(1)−C(7)−C(8)	57.1(2)	N(2)−C(10)−C(11)−C(12)	−178.0(2)
C(1)−C(2)−C(3)−C(4)	−1.5(2)	C(2)−C(1)−C(7)−C(8)	−119.8(2)	C(10)−C(11)−C(12)−C(7)	−1.4(2)
C(14)−C(2)−C(3)−C(4)	173.9(2)	C(6)−C(1)−C(7)−C(12)	−121.3(2)	C(10)−C(11)−C(12)−C(13)	175.9(1)
C(2)−C(3)−C(4)−C(5)	0.1(2)	C(2)−C(1)−C(7)−C(12)	61.8(2)	C(8)−C(7)−C(12)−C(11)	3.6(2)
C(2)−C(3)−C(4)−N(1)	−175.1(2)	C(12)−C(7)−C(8)−C(9)	−2.4(2)	C(1)−C(7)−C(12)−C(11)	−178.0(1)
C(3)−C(4)−C(5)−C(6)	1.0(2)	C(1)−C(7)−C(8)−C(9)	179.1(2)	C(8)−C(7)−C(12)−C(13)	−173.6(1)
N(1)−C(4)−C(5)−C(6)	176.2(1)	C(7)−C(8)−C(9)−C(10)	−1.1(2)	C(1)−C(7)−C(12)−C(13)	4.8(2)

Table 10. Atomic Coordinates ($\times 10^4$) and Equivalent Isotropic Displacement Parameters ($Å^2 \times 10^3$) for BFBZ[a]

	x	*y*	*z*	U_{eq}		*x*	*y*	*z*	U_{eq}
N	3151(1)	4397(3)	5041(1)	29(1)	C(3)	4583(1)	2987(3)	5794(1)	23(1)
F(1)	6910(1)	2536(2)	6486(1)	39(1)	C(4)	3704(1)	4325(3)	5722(1)	22(1)
F(2)	6082(1)	−165(2)	5947(1)	43(1)	C(5)	3335(1)	5449(3)	6358(1)	26(1)
F(3)	6095(1)	93(2)	7154(1)	41(1)	C(6)	3842(1)	5260(3)	7042(1)	24(1)
C(1)	4728(1)	3951(3)	7126(1)	20(1)	C(7)	6026(1)	1325(3)	6522(1)	26(1)
C(2)	5090(1)	2800(3)	6484(1)	20(1)					

[a] U_{eq} is defined as one-third of the trace of the orthogonalized $\mathbf{U}_{ij}$ tensor.

Table 11. Bond Lengths (Å) and Angles (deg) for BFBZ[a]

N−C(4)	1.400(2)	F(3)−C(7)	1.331(2)	C(2)−C(3)	1.389(2)	H(1A)#1..N#2	2.496(1)
N−H(1A)	0.885	C(1)−C(6)	1.386(2)	C(2)−C(7)	1.487(2)	N#1..N#2[b]	3.374(2)
N−H(1B)	0.891	C(1)−C(2)	1.397(2)	C(3)−C(4)	1.386(2)	H(5A)#3..F(3)#1	2.493(2)
F(1)−C(7)	1.347(2)	C(1)−C(1)#1	1.497(3)	C(4)−C(5)	1.86(2)	C(5)#3..F(3)#1[b]	3.849(2)
F(2)−C(7)	1.340(2)			C(5)−C(6)	1.378(2)		

C(6)−C(1)−C(2)	117.2(1)	C(4)−C(3)−C(2)	120.8(2)	H(1A)−N−C(4)	112.6(1)	F(3)−C(7)−F(1)	105.5(1)
C(6)−C(1)−C(1)#1	118.9(2)	C(3)−C(4)−C(5)	118.5(1)	H(1B)−N−C(4)	113.89(9)	F(2)−C(7)−F(1)	105.1(1)
C(2)−C(1)−C(1)#1	123.9(2)	C(3)−C(4)−N	121.0(2)	C(6)−C(5)−C(4)	120.5(2)	F(3)−C(7)−C(2)	113.9(1)
C(3)−C(2)−C(1)	121.0(2)	C(5)−C(4)−N	120.4(2)	C(5)−C(6)−C(1)	122.1(2)	F(2)−C(7)−C(2)	112.8(1)
C(3)−C(2)−C(7)	118.0(1)	H(1A)−N−H(1B)	113.48	F(3)−C(7)−F(2)	106.2(1)	F(1)−C(7)−C(2)	112.6(1)
C(1)−C(2)−C(7)	121.1(1)						

[a] Symmetry transformations used to generate equivalent atoms: #1 = $-x + 1$, y, $-z + 3/2$; #2 = $1/2 + x$, $1/2 + y$, $3/2 - z$; #3 = x, $-1 + y$, z. [b] Not an interaction but noted for precision sake.

Table 12. Selected Torsion Angles (deg) for BFBZ[a]

C(6)−C(1)−C(1)#1−C(6)#1	−101.8(3)	C(1)−C(2)−C(3)−C(4)	0.0(2)	C(2)−C(1)−C(6)−C(5)	−0.4(2)
C(6)−C(1)−C(1)#1−C(2)#1	74.6(1)	C(7)−C(2)−C(3)−C(4)	179.7(2)	C(1)#1−C(1)−C(6)−C(5)	176.2(2)
C(2)−C(1)−C(1)#1−C(2)#1	−109.1(3)	C(2)−C(3)−C(4)−C(5)	−0.8(2)	C(3)−C(2)−C(7)−F(3)	−140.2(2)
C(6)−C(1)−C(2)−C(3)	0.6(2)	C(2)−C(3)−C(4)−N	−175.6(2)	C(1)−C(2)−C(7)−F(3)	39.5(2)
C(1)#1−C(1)−C(2)−C(3)	−175.9(1)	C(3)−C(4)−C(5)−C(6)	0.9(2)	C(3)−C(2)−C(7)−F(2)	−19.0(2)
C(6)−C(1)−C(2)−C(7)	−179.1(2)	N−C(4)−C(5)−C(6)	175.8(2)	C(1)−C(2)−C(7)−F(2)	160.6(1)
C(1)#1−C(1)−C(2)−C(7)	4.5(2)	C(4)−C(5)−C(6)−C(1)	−0.3(3)	C(3)−C(2)−C(7)−F(1)	99.7(2)
				C(1)−C(2)−C(7)−F(1)	−80.6(2)

[a] Symmetry transformations used to generate equivalent atoms: #1 = $-x + 1$, y, $-z + 3/2$.

Table 13. Viscosity and Solubility of Polyimides Derived from Substituted Benzidines

diamine	dianhydride[a]	$[\eta]$,[b] dL/g	solubility	diamine	dianhydride[a]	$[\eta]$,[b] dL/g	solubility
TMBZ	PMDA	insoluble	insoluble	DMBZ	HFDA	0.87	*m*-cresol, TCE
TMBZ	BTDA	1.6	*m*-cresol, TCE, NMP	DMBZ	DSDA	0.65	*m*-cresol, TCE
TMBZ	ODPA	1.4	*m*-cresol, TCE, NMP	DMBZ	BPDA	insoluble[c]	insoluble[c]
TMBZ	HFDA	1.6	*m*-cresol, TCE, NMP	BFBZ	PMDA	insoluble	insoluble
TMBZ	DSDA	1.3	*m*-cresol, TCE, NMP	BFBZ	BTDA	1.6[d]	*m*-cresol
TMBZ	BPDA	5.0	*m*-cresol, TCE	BFBZ	ODPA	1.1[d]	*m*-cresol, TCE,[e] NMP[f]
DMBZ	PMDA	insoluble	insoluble	BFBZ	HFDA	1.9[d]	*m*-cresol, TCE, NMP
DMBZ	BTDA	insoluble	insoluble	BFBZ	DSDA	1.0[d]	*m*-cresol, TCE
DMBZ	ODPA	insoluble	insoluble	BFBZ	BPDA	4.9[d]	*m*-cresol

[a] PMDA = pyromellitic dianhydride; BTDA = 3,3′,4,4′-benzophenonetetracarboxylic dianhydride; ODPA = 4,4′-oxydiphthalic anhydride; HFDA = 4,4′-(hexafluoroisopropylidene)diphthalic anhydride; DSDA = 3,3′,4,4′-diphenylsulfonetetracarboxylic dianhydride; BPDA = 3,3′,4,4′-biphenyltetracarboxylic dianhydride. [b] Intrinsic viscosities were measured in *m*-cresol at 30 °C. [c] The polyimide based on BPDA/DMBZ precipitated from *m*-cresol prematurely during the polymerization; however, the polymerization could be achieved in boiling *p*-chlorophenol (bp = 220 °C, mp = 43−45 °C) to yield polyimides with intrinsic viscosity $[\eta]$ = 10 dL/gm in *p*-chlorophenol at 60 °C (ref 20). [d] $[\eta]$ and solubility were taken from ref 17. [e] TCE = 1,1,2,2-tetrachloroethane. [f] NMP = *N*-methyl-2-pyrrolidinone.

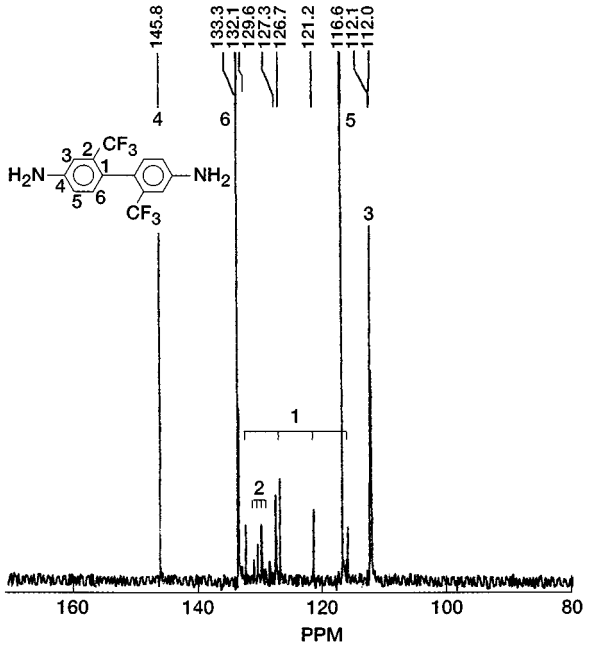

Figure 5. ^{13}C-NMR spectra of 2,2′-bis(trifluoromethyl)benzidine (BFBZ).

Table 14. ^{13}C Assignment for Substituted Benzidines

	DMBZ	TMBZ	BFBZ
C-1	130.70	130.58	127.34
C-2	137.25	137.16	129.94(q)
C-3	112.30	114.24	112.02
C-4	144.98	144.56	145.80
C-5	116.30	(114.24)	116.63
C-6	132.06	(137.16)	133.34
CH_3	19.88	19.90	
CF_3			123.95(q)

Table 15. Physical Properties of Polyimides Based on Substituted Benzidines

property	TMBZ−BPDA	DMBZ−BPDA	BFBZ−BPDA
T_g by TMA[a] (°C)	315	300	290
TGA/N_2 (5% wt loss, °C)	520	500	600
tensile modulus (GPA)[b]	75	150	130
tensile strength (GPa)[b]	2.0	3.5	3.2
elongation at break (%)[b]	2.7	4.0	4.0
density (g/cm^3)	1.37	1.40	1.45

[a] T_g was determined by thermal mechanical analysis (TMA) on a single fiber under different stresseses (σ), by extrapolation to $\sigma = 0$ as described in ref 11. [b] Data were obtained from ref 21.

as their ^{1}H-NMR for CH_3 substituents ($\delta = 1.82$ for TMBZ and 1.97 for DMBZ in $CDCl_3$). The two CF_3 groups in BFBZ are on the opposite side of the $x-z$ plane (anti) containing two amino nitrogens as predicted in terms of the lower energy state by reported molecular modeling;[9,10] however, the two CH_3 groups in DMBZ are unexpectedly located on the same side of the $x-z$ plane (syn), although the two phenyl rings are twisted out of the plane. The torsional angles measured by X-ray crystallography for DMBZ and BFBZ ($\phi = 75°$ and 59°, respectively) are in contrast to the dihedral angles predicted by previous molecular modeling, which indicated that the lowest energy conformations were achieved in noncoplanar biphenyl derivatives when the dihedral angles of two phenyl rings were close to 90° or 270°.[9,10,21] More surprisingly, all the molecular modelings have failed to anticipate that the two CH_3 groups in DMBZ would be located on the same side (syn) of the $x-z$ plane. All the modeling inherently places the substituents at the 2,2′-position on the opposite (anti) to yield the lower energy conformation. One might explain after the fact that the reason that two CF_3 substituents would occupy the opposite sides (anti) on two phenyl rings is due to the balance of dipole moments on BFBZ, which lowers the potential energy as well as steric hindrance due to the slightly larger size of the F atom relative to the H atom. Additionally, the C−F bond length in BFBZ is 1.3 Å, relative to the C−H bond length of 1.1 Å in DMBZ. However, the fact that two CH_3 groups occupied the same side (syn) is still beyond expectation.

Table 13 indicates that TMBZ-based polyimides are generally more soluble than DMBZ and BFBZ containing polyimdes in organic solvents, such as NMP, *m*-cresol, or 1,1,2,2-tetrachloroethane. This phenomenon might be explained in terms of the greater free volume between TMBZ−BPDA polymer chains relative to BFBZ−BPDA and DMBZ−BPDA. The larger torsional angle and the four CH_3 on both sides of the $x-z$ plane in TMBZ inevitably would occupy a bigger volume, relative to the two CH_3 on the adjacent side of DMBZ. The unit cell data ($V = 4149.2$ Å^3 per 13 formula units for TMBZ, $V = 2311.4$ Å^3 per 8 formula units for DMBZ, $V = 1334.95$ Å^3 per 4 formula units for BFBZ) show that the volume per formula unit decreases in the order of TMBZ > BFBZ > DMBZ. However, the real proof of actual free volume for these polyimdes would require the X-ray single crystal structures of the corresponding polymers. Furthermore, the improved solubility of BFBZ−BPDA over DMBZ−BPDA also is attributed to the enhanced organosolubility of CF_3 group over CH_3, since the torsional angle between the two phenyl rings on BFBZ is smaller than that of DMBZ. The small torsional angle in BFBZ ($\phi = 59°$) *versus* $\phi = 75°$ in DMBZ reflects the fact that the two CF_3 substituents were far apart from each other, relative to the two CH_3 groups located adjacent to each other with significant steric hindrance.

As shown in Table 15, the glass transition temperatures (T_g) of polyimides derived from substituted benzidines and BPDA decrease in the order of

TMBZ−BPDA > DMBZ−BPDA > BFBZ−BPDA

The steric hindrance of the four methyl substituents on the two phenyl rings of TMBZ apparently contribute to a higher rotational barrier to the polymer chains during the glass transition state, relative to that of the 2,2′-substituted DMBZ and BFBZ. Furthermore, the two adjacent methyl groups on DMBZ certainly create a higher rotational barrier than that of the two CF_3 groups that were far apart. The thermal gravimetric analysis (TGA) indicated that the CF_3 substituent exhibited higher thermo-oxidative stability than CH_3. The better tensile properties of DMBZ−BPDA over TMBZ−BPDA and BFBZ−BPDA are in part due to the fact that DMBZ−BPDA had highest molecular weight, resulting from the polymerization in higher boiling *p*-chlorophenol. The reported intrinsic viscosities are for DMBZ−BPDA [η] = 10 dL/g in *p*-chlorophenol[20] at 60 °C *versus* [η] = 5.0 dL/g for TMBZ−BPDA and [η] = 4.9 dL/g for BFBZ−BPDA in *m*-cresol at 30 °C. Additionally, the electron-donating CH_3 groups on DMBZ could increase the nucleophilicity of DMBZ relative to the electron-withdrawing CF_3 in BFBZ, thus resulting in the higher molecular weight and higher viscosity for DMBZ−BPDA polyimide. Moreover, the slower crystallization rate which promotes higher crystal orientation and draw ratio, as displayed by DMBZ−BPDA during

the drawing process, could also contribute to its higher tensile properties.[22,23] However, BFBZ−BPDA exhibits higher degradation temperature (T_d = 600 °C) than either TMBZ−BPDA or DMBZ−BPDA (Table 15), because CF_3 substituents are thermally more stable than CH_3.

Summary and Conclusions

Polyimides prepared from 2,2′,6,6′-tetrasubstituted 4,4′-biphenyldiamine exhibit enhanced solubility relative to 2,2′-disubstituted benzidine, due to the larger torsional angle between two phenyl rings as revealed by X-ray crystallography (ϕ = 83° for TMBZ, ϕ = 75° for DMBZ, and ϕ = 59° for BFBZ). Unexpectedly, the two CH_3 groups on DMBZ were located on the same side (syn) of the $x-z$ plane in an adjacent location whereas the two CF_3 substituents on BFBZ were far apart on the opposite side (anti) of the $x-z$ plane. Furthermore, the CF_3 substituents impart not only better thermooxidative stability but also increased solubility in the resulting polyimides, relative to CH_3 groups.

Acknowledgment. The authors thank Dr. Makoto Kaji of Hitachi, Japan, for providing a small quantity of 2,2′-dimethylbenzidine for X-ray crystallography.

Supporting Information Available: Tables of H atom coordinates and isotropic displacements for 2,2′,6,6′-tetramethylbenzidine (TMBZ), for 2,2′-dimethylbenzidine (DMBZ), and for 2,2′-bis(trifluoromethyl)benzidine (BFBZ) (9 pages); observed and calculated structure factors for TMBZ, DMBZ, and BFBZ (21 pages). Ordering information is given on any current masthead page.

References and Notes

(1) Blair, T. I.; Morgan, P. M.; Killian, F. L. *Macromolecules* **1977**, *10* (6), 1396.
(2) Percha, Im J.; Yeakle, D. S. *Mater. Res. Soc. Symp. Proc. (Mater. Sci. Eng. Rigid-Rod Polym.)* **1989**, *234*, 307.
(3) Navarro, F. *Macromolecules* **1991**, *24*, 6622.
(4) Morgan, P. M. *Macromolecules* **1977**, *10* (6), 1381.
(5) Becker, K. H.; Schmidt, H-W. *Macromolecules* **1992**, *25*, 6784.
(6) Bhowmik, P. K.; Atkin, E. D. T.; Lenz, R. W. *Macromolecules* **1993**, *26*, 440.
(7) Schmidt, H.-W.; Guo D. *Makmol. Chem.* **1988**, *189*, 2029.
(8) Rogers, H. G.; Gaudiana, R. A.; Hollinsed, W. C.; Kalyanaraman, P. S.; Manello, J. S.; McGrown, C.; Minns, R. A.; Sahatjian, R. *Macromolecules* **1985**, *18*, 1058.
(9) Tsuzuki, S.; Tanabe, K.; Nagawa, Y.; Nakanishi, H. *J. Mol. Struct.* **1988**, *178*, 277.
(10) Coburn, J. C.; Soper, P. D.; Auman, B. C. *Macromolecules* **1995**, *28*, 3253.
(11) Wu, T. M.; Chvalun S.; Blackwell, J.; Cheng, S. Z. D.; Wu, Z.; Harris, F. W. *Polymer* **1995**, *36* (11), 2123.
(12) Eashoo, Mark; Shen, D.; Wu, Z.; Lee, C. J.; Harris, F. W.; Cheng, S. Z. D. *Polymer* **1993**, *15*, 3209.
(13) Cheng, S. Z. D.; Lee, S. K.; Barley, J. S.; Hsu, S. L. C.; Harris, F. W. *Macromolecules* **1991**, *24*, 1883.
(14) Cheng, S. Z. D.; Arnold, F. E.; Zhang, A.; Hsu, S. L. C.; Harris, F. W. *Macromolecules* **1991**, *24*, 5856.
(15) Matsuura, T.; Hasuda, Y.; Nishi, S.; Yamada, N. *Macromolecules* **1991**, *24*, 5001.
(16) Chuang, K. C.; Vannucci, R. D.; Ansari, I.; Cerny, L. L.; Scheiman, D. A. *J. Polym. Sci. Chem. Ed.* **1994**, *32*, 1341.
(17) Chuang, K. C. *High Perform. Polym.* **1995**, *7*, 81.
(18) Harris, F. W.; Hsu, S. L. C.; Tso, C. C. *Polym. Prepr.* **1991**, *32* (2), 97.
(19) Cheng, S. Z. D.; Wu Z.; Eashoo, M.; Hsu, S. L. C.; Harris, F. W. *Polymer* **1991**, *32* (10), 1803.
(20) Eashoo, M.; Wu, Z.; Zang, A.; Shen, D.; Tse, C.; Harris, F. W.; Cheng, S. Z. D. Mac*omol. Chem. Phys.* **1994**, *195*, 2207.
(21) Arnold, F. E., Jr.; Bruno, K. R.; Shen, D.; Eashoo, M.; Harris F. W.; Cheng, S. Z. D. *Polym. Eng. Sci.* **1996**, *33* (21), 1373.
(22) Cheng, S. Z. D.; Wu, Z.; Hull, D. L.; Chuang, K. C. *HiTemp Rev.* ***1995****, NASA CP 10178*, vol. 1, Article 6.
(23) Wu, Z.; Zhang, A.; Shen, D.; Leland, M.; Harris, F. W.; Cheng, S. Z. D. *J. Thermal. Anal.* **1996**, *46* (3-4), 719.
(24) Copyright 1989, 1990, Siemens Analytical X-Ray Instruments, Inc., Madison, WI.
(25) Sheldrick, G. M. *SHELXL-93 Program for the refinement of crystal structures.* University of Gottingen, Germany, 1993.
(26) An extinction parameter, x, is defined where F_c is multiplied by $k[1 + 0.001 \times F_c^2\lambda^3/\sin(2\theta)]^{-1/4}$ with k = overall scale factor.
(27) $wR2 = [\sum[w(F_o^2 - F_c^2)^2]/\sum[w(F_o)^2]^2]^{1/2}$. Weighted R-factors are based on F^2 and are statistically about twice as large as those based on F.
(28) $R1 = \sum||F_{0^\circ}| - |F_c||/\sum|F_{0^\circ}|$. Conventional R-factors are calculated using the observed criterion. This criterion is irrelevant to the choice of reflections used in the refinement.
(29) $S = [\sum[w(F_{0^\circ}^2 - F_c^2)^2]/(n - p)]^{1/2}$. The goodness-of-fit is based on F^2 where n = number of data and p = number of parameters refined.

MA970309B